EVS24
Stavanger, Norway, May 13-16, 2009

An integrated approach to high-power battery modeling: from the electrochemistry to the vehicle

V. Sauvant-Moynot[1], E. Prada[2], J. Bernard[3], J. Martin[4], A. Sciarretta[5], N. Rajapakse[6], Y. Touzani[7], J-C. Dabadie[8], F. Badin[9]

[1]*Corresponding author, IFP Lyon, BP3, 69369 Solaize, France ; valerie.sauvant@ifp.fr*
[2]*IFP Lyon, BP3, 69369 Solaize, France ; eric.prada@ifp.fr*
[3]*IFP Lyon, BP3, 69369 Solaize, France ; julien.bernard@ifp.fr*
[4]*IFP Lyon, BP3, 69369 Solaize, France ; joseph.martin@ifp.fr*
[5]*IFP , 3-4 avenue de Bois-Préau, 92852 Rueil-Malmaison, France ; antonio.sciarretta@ifp.fr*
[6]*IFP , 3-4 avenue de Bois-Préau, 92852 Rueil-Malmaison, France*
[7]*IFP , 3-4 avenue de Bois-Préau, 92852 Rueil-Malmaison, France ; youssef.touzani@ifp.fr*
[8]*IFP , 3-4 avenue de Bois-Préau, 92852 Rueil-Malmaison, France ; J-Charles.dabadie@ifp.fr*
[9]*IFP, 3-4 avenue de Bois-Préau, 92852 Rueil-Malmaison, France; francois.badin@ifp.fr*

Abstract

Due to their physical basis, battery lumped electrochemical and thermal models arise as a promising alternative to popular equivalent circuit models to predict battery behaviours. In this paper, our objective is to present an advanced 0D-electrochemical and thermal model of a Ni-MH cell recently calibrated to describe a 6,5 Ah, 168 cells, 202V nominal Ni-MH commercial battery pack and to highlight the benefits of an integrated modeling approach from electrochemistry to various applications: battery performance characterisation, control-law development and hybrid vehicle simulation.

After a synthetic presentation of the advanced 0D electrochemical and thermal Ni-MH cell model, the first part of the paper will be devoted to the recent work on model developments and parameter tuning to account for the voltage evolution at various temperatures and current levels, but also for the thermal and pressure evolutions in the cell. Then, promising applications of the model are discussed. First, the physics-based modeling of traction battery offers an opportunity to discuss the mechanisms of ageing along the operating life. Secondly, the advanced Ni-MH lumped-parameter model -where the state of charge (SoC) is an internal parameter- can be used to design an extended Kalman filter and provide a fairly accurate and real-time indication of the battery SoC on-board. Thirdly, the 0D electrochemical model can be integrated into a vehicle simulator to optimise the HEV architecture or quantify energy fluxes, while reflecting the battery physics properly.

As a main conclusion, it is worth noting that the Ni-MH battery model is detailed as a case study, but this integrated approach can be applied to any Li-ion technologies.

Keywords: battery model, BMS, state of charge, simulation, HEV

1 Introduction

The operation of high-power batteries in hybrid electric vehicles (HEV) requires to furnish and absorb large current spikes almost instantaneously. The various aspects of performance required from a battery in terms of power and energy can be assessed experimentally [1] but the battery modeling can be of valuable use to explore pulse power limitations and thermal behaviour of a candidate technology [2]. Due to their physical basis, battery lumped electrochemical and thermal models arise as a promising alternative to popular equivalent circuit models to predict battery behaviours [3]. An improved electrochemical and thermal lumped-parameter model for a sealed Ni-MH cell was recently proposed by our group [4] in order to better approach the outcome of 1D models, while keeping the same level of complexity of standard 0D models and avoiding excessive computational time. Besides being useful for physical understanding and diagnosis, the so called lumped-parameter electrochemical model was developed as a computationally efficient approach to design an extended Kalman filter and provide a fairly accurate and real-time indication of the battery state-of-charge on-board. Moreover, the advanced 0D electrochemical model can be integrated into a vehicle simulator to optimise the HEV architecture or quantify energy fluxes while reflecting the battery physics properly.

The Ni-MH lumped-parameter model developed in the AMESim simulation environment was calibrated on a 6,5 Ah, 1,2 V nominal Ni-MH commercial cell and validated against 1C charge / discharge and hybrid pulse power characterisation (HPPC) tension data sets at 20°C collected on a Prius 2 Ni-MH battery pack, assuming that cell construction, SoC and temperature are uniform throughout the serial pack [4]. In that case, the battery was characteristic of the "beginning-of-life" since it was a new one which was not used in a vehicle.

After a synthetic presentation of the advanced 0D electrochemical and thermal Ni-MH cell model, the first part of the paper will be devoted to the recent work on model developments and parameter tuning to account for the voltage evolution at various temperatures and current levels, but also for the thermal and pressure evolutions. In a second part, the benefits of an integrated modeling approach based on electrochemistry is highlighted for the battery ageing diagnosis, for the control-law development and for the hybrid vehicle simulation.

2 Electrochemical and thermal 0D Ni-MH cell model

A Ni-MH cell is a dual-intercalation electrochemical system in which proton insertion in the positive solid nickel electrode and hydrogen de-insertion in the negative solid metal/hydride electrode occur during discharge and vice versa during charge. Electrochemical reactions taking place at the electrode/electrolyte interface (assuming discharge) are:

$$NiOOH + H_2O + e^- \leftrightarrow Ni(OH)_2 + OH^- \quad (1)$$

$$½\ O_2 + H_2O + 2e^- \leftrightarrow 2OH^- \quad (2)$$

at the positive electrode and

$$M + H_2O + e^- \leftrightarrow MH + OH^- \quad (3)$$

$$½\ O_2 + H_2O + 2e^- \leftrightarrow 2OH^- \quad (4)$$

at the negative electrode.

Side equations (2) and (4) constitute the oxygen re-circulation inside the cell. The oxygen is transported from one electrode to the other via the liquid electrolyte and, after exceeding its solubility limit in the electrolyte, via a gas phase. Thus a Ni-MH cell is a three-phase system, with one gas phase besides the solid matrices and the liquid electrolyte. The accumulation of oxygen in the gas phase increases the cell pressure in the gas reservoir above the cell (constant volume).

2.1 Advanced 0D model formulation

The lumped-parameter description is based on the assumption of considering the concentrations of the active species as homogeneous within the battery, i.e. spatial gradients are neglected. Moreover, the concentration of the hydroxyls ions in the electrolyte is taken as a constant. Consequently, the model state equations are given by the mass balance equations of the remaining active species. The mass flows involving the three active species are related to the current densities of the main and side electrochemical reactions (equations 5). The diffusion into a single solid particle is accounted for by an equation based on the superposition integral [5]. Then the bulk concentration for each species is distinguished from the interfacial concentration, both being functions of time. The current densities are calculated using the Butler-Volmer equations (equations 6) as a function of the species interfacial concentrations, the potential differences at the solid-liquid interface on the electrodes, and

the equilibrium potentials (open-circuit potentials) of the reactions (equations 7). Current balance equations (8) provide the missing relationships between the reaction current densities, the potential differences, the cell voltage, and the cell current. Among other refinements, two double-layer capacitances are introduced in the charge balance equation to account for the electrolyte ionic species accumulation at both electrode interfaces due to the diffusion gradient. Moreover, the typical hysteresis effect of Ni-MH batteries is taken into account through a non ideal expression of the thermodynamic equilibrium potential. In the model, thermal effects are adequately taken into account by introducing an energy balance equation for the whole cell (equations 9). Heat production due to irreversibility in the reactions, heat losses through the cell external surface, as well as energy accumulation in the cell are the terms of such equation. Cell temperature affects the reaction and diffusion kinetics.

Main equations of the advanced 0D model summarised in Table 1 are detailed elsewhere, together with the calibration method on a 6,5 Ah, 1,2 V nominal Ni-MH commercial cell [4].

Table1: Main equations of the advanced 0D electrochemical model [4]

Physics	Mathematical expressions	
Mass balance	$$\frac{dc_{Ni}}{dt} = -\frac{J_1}{l_{y,pos}F}$$ $$\frac{dc_{MH}}{dt} = -\frac{J_3}{l_{y,neg}F}$$ $$\frac{dp_{O2}}{dt} = \frac{10RT}{V_{gas}} \cdot \frac{S_{pos}J_2 + S_{neg}J_4}{4F}$$	(5)
Kinetics	$$J(t) = J_0 \left\{ \frac{\prod_{j=1}^{N'} [P_j]_t^{o_{Pj}}}{\prod_{j=1}^{N'} [P_j]_{eq}^{o_{Pj}}} \exp\left(\frac{\alpha_{ox} nF\eta(t)}{RT}\right) - \frac{\prod_{i=1}^{N} [R_i]_t^{o_{Ri}}}{\prod_{i=1}^{N} [R_i]_{eq}^{o_{Ri}}} \exp\left(-\frac{\alpha_{red} nF\eta(t)}{RT}\right) \right\} \exp\left(\frac{E_a}{R}\left(\frac{1}{T} - \frac{1}{T_0}\right)\right)$$	(6)
Equilibrium potentials	$$\eta_1 = \Delta\Phi_{pos} - \left(\left(1 - 2\frac{\bar{c}_{Ni}}{c_{Ni,max}}\right) K_{inter}\frac{RT}{F} + (T - T_0)\frac{dU_1}{dT} + U_{eq,ref,1}\right)$$ $$\eta_2 = \Delta\Phi_{pos} - \left(U_{0std,2} + (T - T_0)\frac{dU_2}{dT}\right)$$ $$\eta_3 = \Delta\Phi_{neg} - \left(U_{0std,3} - \frac{RT}{F}\mu\ln(c_{MH,ref}) + (T - T_0)\frac{dU_3}{dT}\right)$$ $$\eta_4 = \Delta\Phi_{neg} - \left(U_{0std,4} + (T - T_0)\frac{dU_4}{dT}\right)$$	(7)
Charge balance	$$\frac{d\Delta\Phi_{pos}}{dt} = \frac{1}{C_{dl,pos}}\left(\frac{I_{cell}}{S_{pos}} - J_1 - J_2\right)$$ $$\frac{d\Delta\Phi_{neg}}{dt} = \frac{1}{C_{dl,neg}}\left(-\frac{I_{cell}}{S_{neg}} - J_3 - J_4\right)$$ $$V_{cell} = \Delta\Phi_{pos} - \Delta\Phi_{neg} + R_{int}I_{cell}$$	(8)
Energy balance	$$\frac{dT}{dt} = \frac{1}{M_{cell}C_p}(\varphi_{gen} - \varphi_{tra})$$ $$\varphi_{gen} = V_{cell}I_{cell} - \sum_{z=1}^{4} J_z\left(U_{0std,z} - T_0\frac{dU_z}{dT}\right)S_{(z)}$$ $$\varphi_{tra} = h_{cell}A_{cell}(T - T_a)$$	(9)

2.2 Advanced 0D model validation

Recent attention was paid to the validation of the model against new experiments to also adjust pressure and thermal parameters and provide a complete voltage/pressure/thermal-behaviours Ni-MH battery model. Considering the pressure increase related to the gaseous oxygen production in charge conditions approaching full or overcharge, the liquid/gas interfacial equilibrium for the oxygen species links the dissolved oxygen concentration to the gaseous oxygen pressure via the Henry law, while the ideal gas law applies in the gas reservoir. An experiment was conducted on a 6,5 Ah 7,2 V nominal voltage Prius 2 Ni-MH module submitted to 1C charge, 30 minutes relaxation and 1C discharge cycles at ambient temperature while monitoring at the same time the voltage, the pressure increase in the gas reservoir on the top of the module thanks to a manometer and the skin temperature increase on one side (Fig. 1). Comparison of experimental and simulated results shown on Fig.2 provides a very satisfactorily agreement. As one can see, full charge and overcharge are accompanied with gaseous production related to a secondary reaction, which is obviously exothermic.

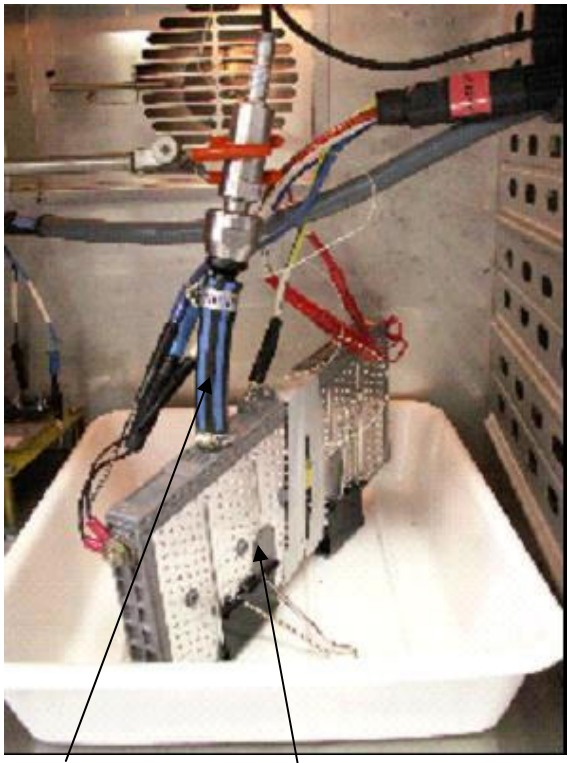

Figure1: Experimental set-up for the parallel measure of tension, pressure and skin temperature on a Prius 2 module at room temperature during 1C charge, 30 minutes relaxation and 1C discharge cycles

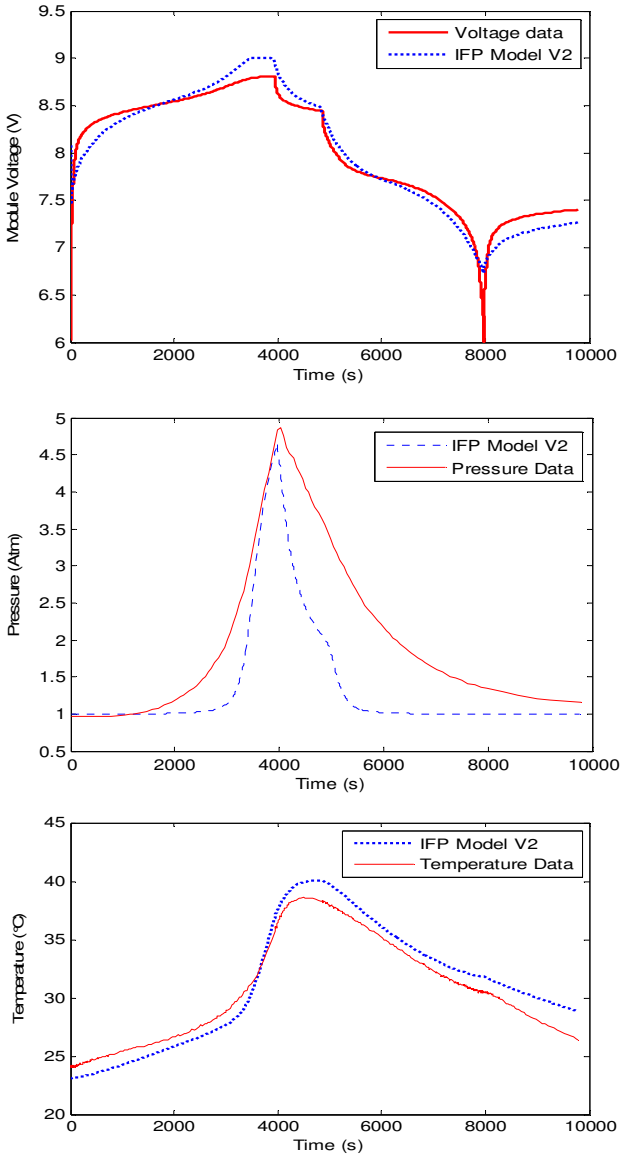

Fig 2: Comparison of measured (red line) and simulated (blue dots) Ni-MH module battery voltage, pressure and skin temperature

To provide additional experimental validation of the refined 0D model over a wide temperature range, the dynamic profile test so called Hybrid Pulse Power Characterisation (HPPC) test was applied to the entire Prius 2 Ni-MH battery pack consisting of 168 serially connected cells [6]. HPPC tests were performed on the battery testing power bench at IFP (500A / 500V / ±120 kW) in isothermal conditions. A specific ventilation was applied to the pack set in a large climatic chamber in order to maintain the internal temperature as close as possible to the temperature set-point of the experiment. Thus, it is assumed that cell construction, SoC, and temperature are uniform throughout the pack: no attempt was made to account for cell-to-cell differences arising from manufacturing variability or temperature distribution within the pack. The complete high current HPPC test consists with a succession of sequences as shown in Fig. 3, including discharge pulse (-130A, 10s) and charge pulse (+85A, 10s) every 10% of SoC from SoC = 110% to 0%. Fig. 4 gives the results for the complete high current HPPC test at 25°C and Fig.5 displays the result for a single profile at intermediate SoC.

The model predictions in these highly dynamic conditions reflect the experimental measurements on the pack very correctly over the entire HPPC test, and relaxation phenomena are particularly well taken into account in the model. Model prediction can be considered as very good at 25°C between SoC =30% to 80% (which is of interest in the traction application), since the relative error between measurements and simulation remains below ±3%. Notice that dynamic periods where discharge and recharge pulses correspond to -25 kW and +17kW are even better reproduced, for which the difference reaches less than 1 %.

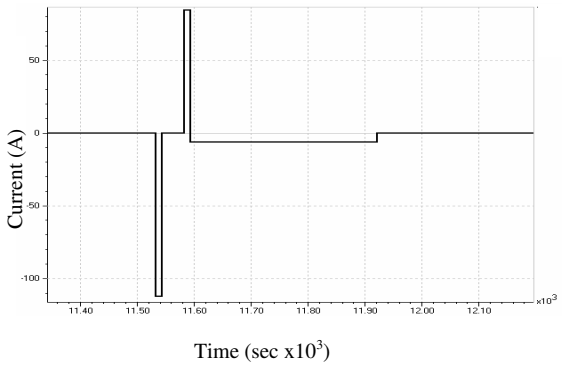

Figure3: High current Hybrid Pulse Power Characterization test profile

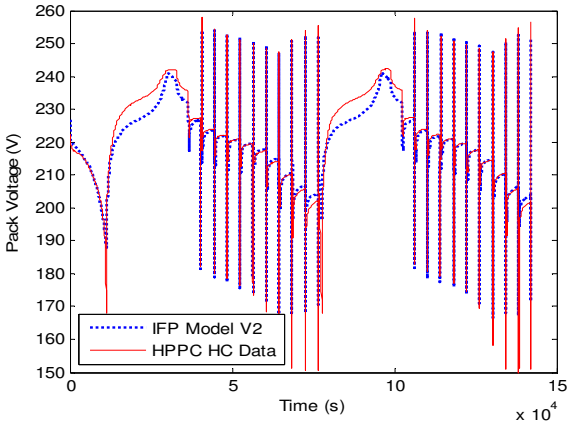

Figure4: Comparison of measured (red line) and simulated (blue dots) Ni-MH battery pack voltage using high current HPPC profiles at 25°C

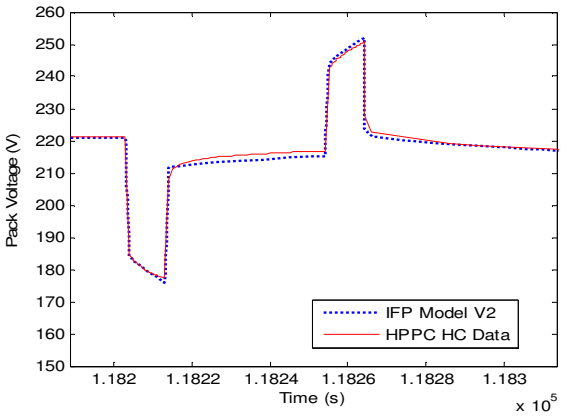

Figure5: Comparison of measured (red line) and simulated (blue dots) Ni-MH battery pack voltage during high current HPPC profiles at 25°C, SoC=50%

The temperature prediction of the 0D advanced model for the complete high current HPPC test at 25°C is also in good agreement with the experiments, as shown on the Fig. 6.

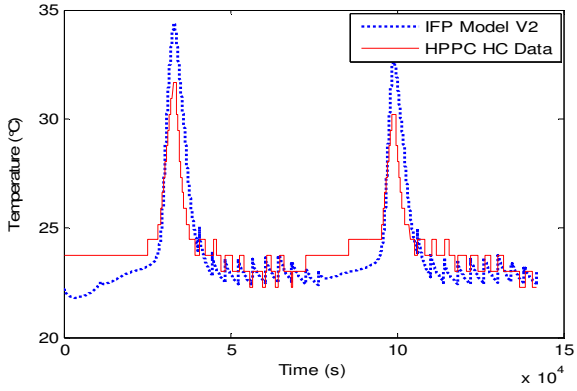

Figure6: Comparison of measured (red line) and simulated (blue dots) Ni-MH battery pack temperature during high current HPPC profiles at 25°C

2.3 Influence of temperature

The model predictability was also studied over a wide temperature range, in particular at lower temperatures which are critical for the traction application. The low current HPPC profiles were applied to the battery pack at 0°C and -25°C, where discharge and recharge pulses correspond to -7.5 kW and +5.5kW. Experimental and simulation results are compared in terms of voltage and temperature, respectively, on Fig. 7 and Fig. 8 at 0°C, on Fig. 9. and Fig. 10 at -25°C. In these difficult conditions, the model predictions reflect the experimental measurements on the pack quite correctly over the entire HPPC test: dynamic periods and relaxation phenomena are still particularly well taken into account in the model, since the relative error between measurements and simulation remains below ±3% between SOC = 80% to 30% at 0°C and -25°C. The temperature prediction remains also fairly good.

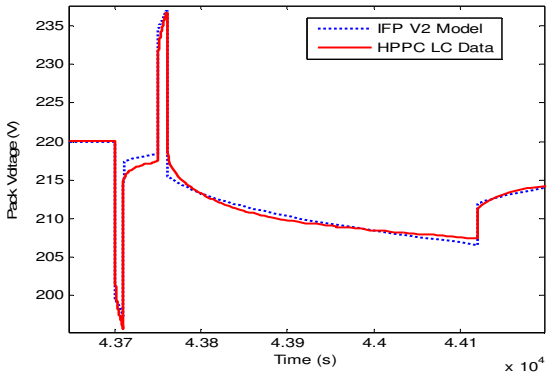

Figure7: Comparison of measured (red line) and simulated (blue dots) Ni-MH battery pack voltage during low current HPPC profiles at 0°C, SoC=50%

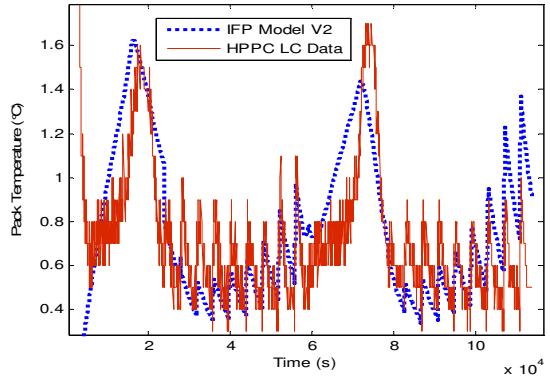

Figure8: Comparison of measured (red line) and simulated (blue dots) Ni-MH battery pack temperature during low current HPPC profiles at 0°C

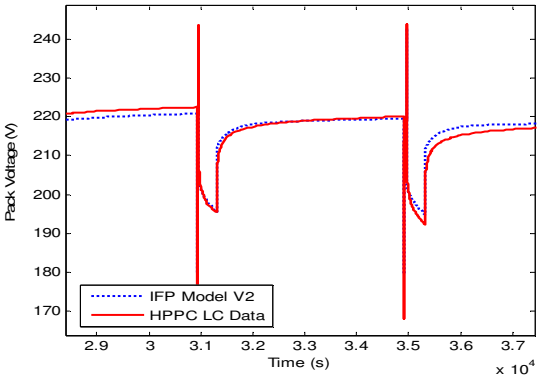

Figure9: Comparison of measured (red line) and simulated (blue dots) Ni-MH battery pack voltage during low current HPPC profiles at -25°C, SoC=50%

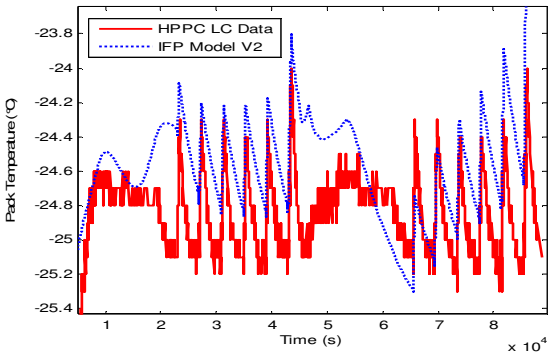

Figure10: Comparison of measured (red line) and simulated (blue dots) Ni-MH battery pack temperature during low current HPPC profiles at -25°C

3 Main applications of the 0D electrochemical and thermal Ni-MH battery model

3.1 Comprehension of ageing mechanisms

The comparison between simulation and experimental results obtained on the "beginning-of-life" characterisation of a new Prius 2 battery pack and so called "in-life" characterisation of another pack used during 3 years in a Prius 2 vehicle was performed to point out the interest of the advanced lumped-parameter Ni-MH battery model to discuss the material evolution in Ni-MH cells during service.

In Ni-MH battery systems, the hydrogen storage alloy at the negative electrode plays an important role with respect to power performance and life duration. Power performance and cycle life behaviour are related to each other by the electrochemical and mechanical properties of the

alloy, via a more or less reciprocal relationship [7]. Consecutive lattice expansion and contraction during hydrogen intercalation and extraction produces mechanical stress, finally leading to the cracking of alloy grains submitted to electrochemical cycles. As a result the particle size of the alloy is reduced (Fig.11) and the surface area of the negative electrode increases, which is profitable for the power performance of the negative electrode in a first step. But the increase of active surface associated with lattice expansion also favours the alloy corrosion in alkaline media, leading to the formation of surface films and a change of the chemical composition, especially in near surface regions of the alloy particles [8].

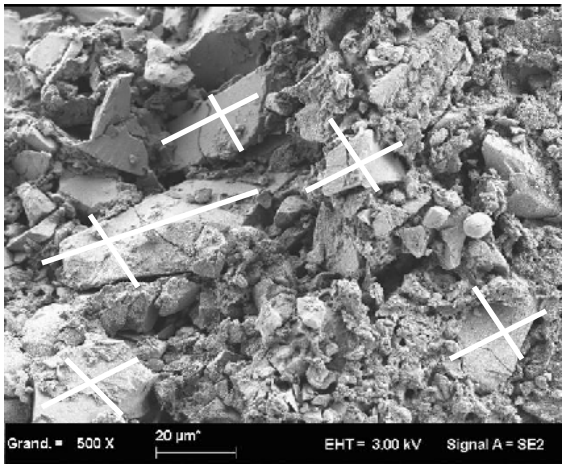

Figure11: SEM of fresh alloy removed from a NiMH 6,5Ah 1,2V cell and schematic representation of the cracking of alloy grains due to electrochemical grinding

Consequently, positive effects due to electrochemical grinding at the negative electrode are expected at an early stage of cell life, as long as corrosion do not become overcompensating. According to the literature, stability against corrosion and pulverisation on one hand and good electrochemical performance on the other hand both depend on the chemical composition of the alloy, its morphological properties and the cycling regime used.

A high current HPPC profile was applied with the IFP power bench at 25°C on a three years old PRIUS 2 battery pack and voltage data were modelled with the Ni-MH electrochemical lumped model (Fig.12). The parameter related to the active surface of the negative electrode was modified to fit experimental data in a satisfactorily way, namely active surface was increased by 130% to take electrochemical grinding and alloy pulverisation into account. So far, electronic exchange current density for negative insertion reaction was not changed, which suggests that there is no significant charge transfer increase due to corrosion layer at this stage. As a matter of fact, the recharge resistance measured on the three years old battery with the high current HPPC was systematically 5 to 15 % lower than the recharge resistance of the new battery. Therefore, positive effects due to alloy particle cracking are observed at this stage as reported in the literature, but corrosion reactions may take profit later from an increase of the surface area of the negative electrode.

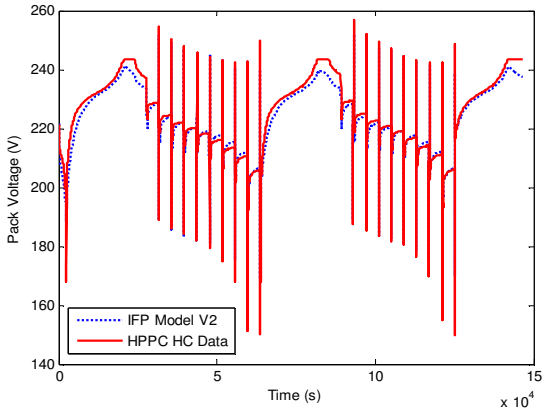

Figure12: Comparison of measured (red line) and simulated (blue dots) voltage on a 3 years old Ni-MH battery pack using high current HPPC profiles at 25°C

3.2 Electrochemical and thermal 0D Ni-MH cell model for control law development

As auxiliary power source, traction batteries in hybrid electric vehicles are operated at a nominal state-of-charge (SoC) level near 50% while staying into a realistic operating window like 30-70% SoC to deal with charge current bursts without going into overcharge or overdischarge. Given this operational constraints imposed on batteries, there is a need for a precise SoC estimation by the battery management system (BMS), as an accurate and reliable indication for the vehicle control system. This quantity is not directly measurable on board, since it is related to the concentration of reactive species inside the battery cells. The coulomb-counting procedure is not reliable for a precise SoC determination in traction batteries since not all current supplied goes to charging the cell and the charge lost to any undesired charge reaction is not included. As a promising solution, battery models based on the physic of the cells can be used to design an extended Kalman filter and provide a fairly accurate indication of the battery

SoC [9]. On the basis of the advanced Ni-MH lumped-parameter model described in the first part, an extended Kalman was designed using Simulink tool as illustrated on the Fig.13.

Validation has been conducted by co-simulation and Fig.14 presents four applications of SoC estimation for an european driving cycle at 20°C (three repetition) to compare results from either model, EKF without noise (ideal), EKF and Coulomb counting. The agreement between EKF and model results under dynamic current solicitation undoubtly assesses the mathematical background and design of the EKF which may be used in a typical BMS algorithms.

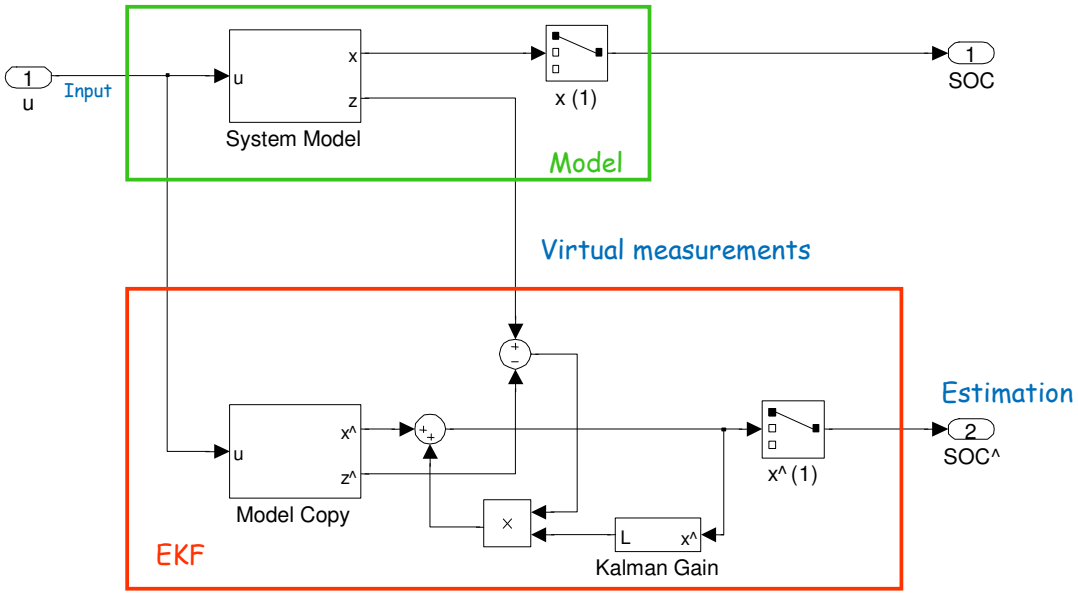

Figure13: EKF design and co-simulation

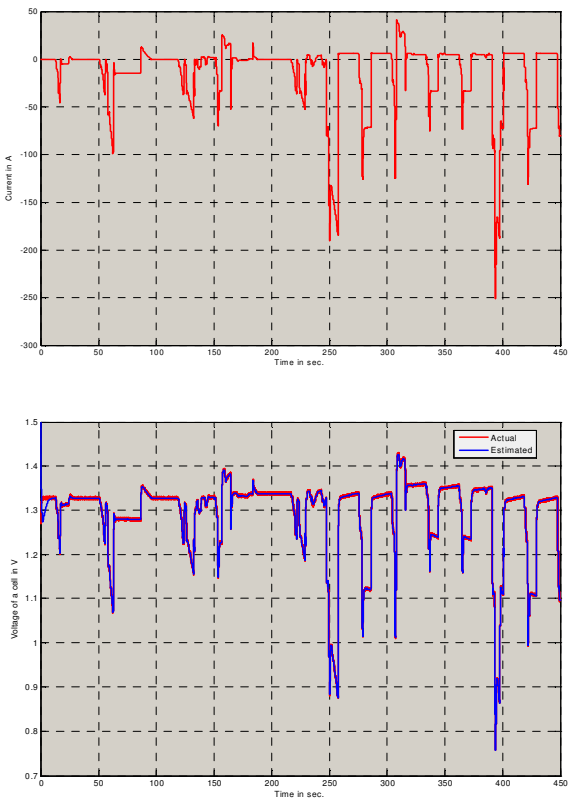

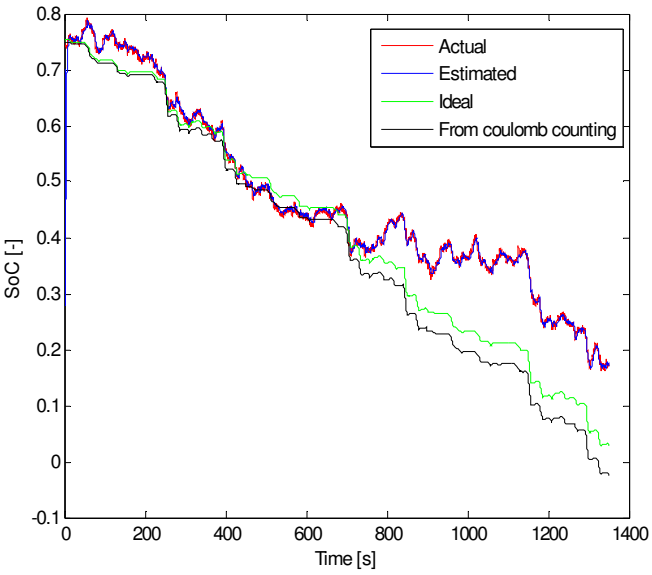

Figure14: Dynamic of current, voltage and SoC estimation results given by 0D modeling (actual), EKF (estimated), EKF without noise (ideal) and from coulomb counting

3.3 Electrochemical and thermal 0D Ni-MH cell model for a HEV simulator

Furthermore, the 0D electrochemical model can be integrated into a vehicle simulator to optimise the HEV architecture or quantify energy fluxes while reflecting the battery physics properly. For example, using the simulator for the Prius 2 vehicle (Fig. 15) developed on the AMESim tool [10], it could be possible to run the Ni-MH battery model with both sets of parameters used previously in the paper, namely for the new battery pack and the 3 years old one ("in-life").

This work is ongoing to discuss the influence of battery ageing and take into account the evolution of battery performance during life on energy fluxes in ordre to optimize the vehicle architecture – whatever the hybridation, from mild to full hybrid, from PHEV to BEV.

4 Conclusions

This paper covers the integrated approach conducted to model high-power battery pack, from electrochemistry to vehicle applications. The main result is the high precision level obtained by our advanced 0D electrochemical model for both voltage and temperature prediction of the Prius 2 battery pack, under strong to zero current, while covering the wide thermal window of the traction application. For it is physics-based, computational efficient and validated against experiments in nominal and extreme operating conditions, this model is of primarily interest to discuss battery performance evolution during ageing, to develop control-law for the BMS, or to design and optimise the vehicle architecture on a VEH simulator.

Furthermore, it is worth noting that the Ni-MH model is detailed as a case study, but this approach is also applied at IFP to Li-ion technologies.

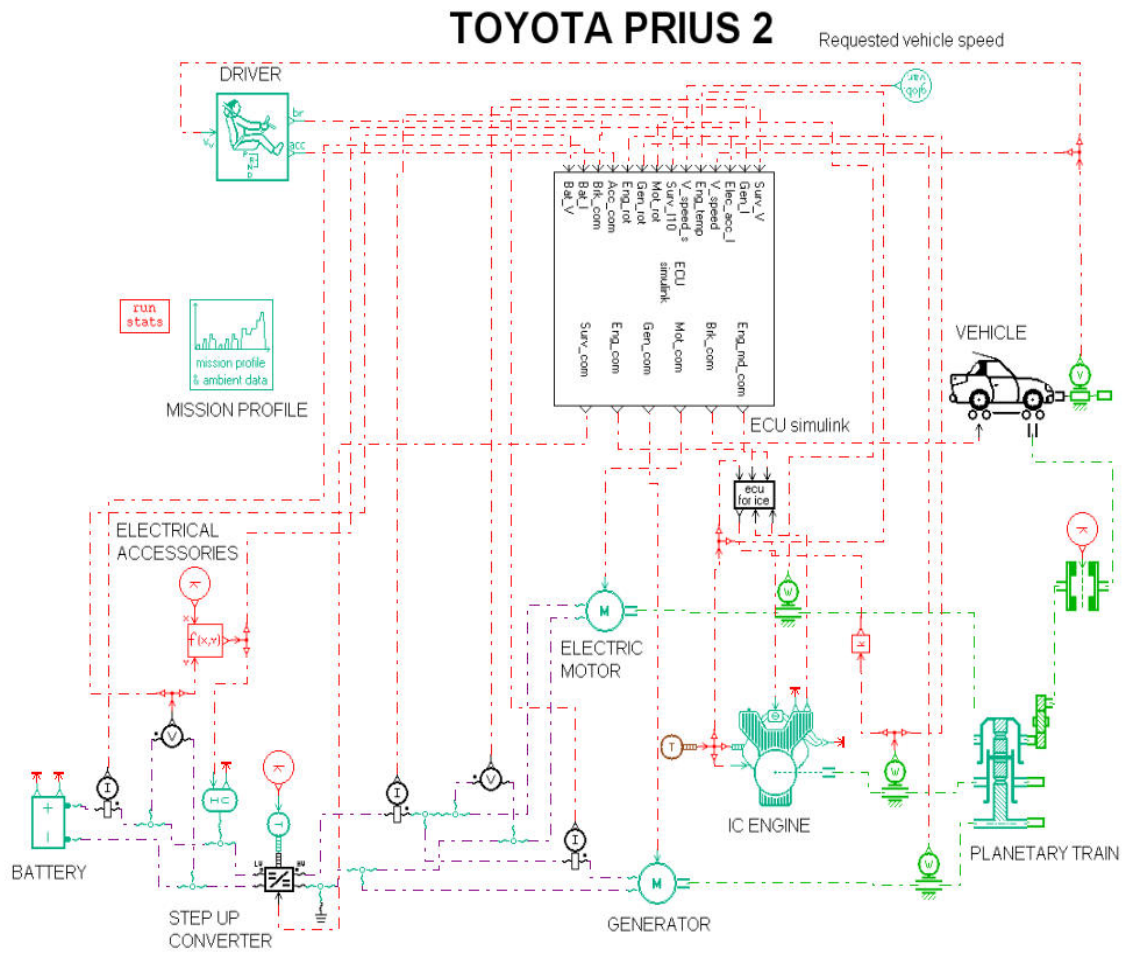

Fig. 15: Prius 2 simulator developed on AMESim tool in the VECSIM project [10].

References

[1] T.Q. Duong, *USABC and PNGV test procedures*, Journal of Power Sources, 89 (2000), 244-248

[2] K. Smith, C.Y. Wang, *Power and thermal characterization of a lithium-ion battery pack for hybrid-electric vehicles,* Journal of Power Sources, 160 (2006), 662-673

[3] A. Sciarretta, V. Sauvant-Moynot, I. Faille, *Advances in model-based SoC determination for HEV traction batteries*, AEA 2008, 4th European Conference on Alternative Energies for the Automotive Industries, paper 13

[4] J. Bernard, A. Sciarretta, Y. Touzani, V. Sauvant-Moynot, *Advances in electrochemical models for predicting the cycling performance of traction batteries: experimental study on Ni-MH and simulation*, Proceeding of Advances in Hybrid Powertrains (2008), 25-26 November, Rueil-Malmaison, France

[5] B. Paxton, J. Newman, *Modeling of nickel/metal hydride batteries*, Journal of the Electrochemical Society, 144 (1997), 3818-3831

[6] FreedomCar Battery Test Manual For Power-assist hybrid Electric vehicle (2003), INEEL/DOE

[7] P. Bauerlein, C. Antonius, J. Loeffler, J. Kümpers, *Progress in high-power nickel–metal hydride batteries*, Journal of Power Sources, 176 (2008), 547–554

[8] P.H.L. Notten, R.E.F. Einerhand, J.L.C. Daams, *How to achieve long-term electrochemical cycling stability with hydride-forming electrode materials*, Journal of Alloys and Compounds, 231 (1995), 604-610

[9] G.L. Plett, *Extended Kalman filtering for battery management systems of LiPB-based HEV battery packs: Part 3. State and parameter estimation*, Journal of Power Sources, 134 (2004), 277-292

[10] A. Albrecht et Al., Synthesis report of VECSIM project (2007), IMAGINE - INRETS - GAZ DE FRANCE - IFP

Authors

IFP is a world-class public-sector research and training center, aimed at developing the technologies and materials of the future in the fields of energy, transport and the environment.

From chemists/electrochemists to control and powertrain simulation engineers, the IFP's staff of battery projects forms a unique network of expertise:

Valérie Sauvant-Moynot joined the Materials Department of IFP in 1999 with an Engineering degree of the Chemical National School of Paris (ENSCP) and a PhD in Polymer Science. She is currently project manager "battery" for the Powertrain Engineering Technology Business Unit.

Eric Prada develops and calibrates models of electrochemical storage systems in AMESim and Simulink environments. He joined the Materials Department of the Applied Chemistry & Physical Chemistry Division in 2008 with an Engineering degree of the Grenoble Electrochemistry National School (ENSEEG).

Julien Bernard is in charge of R&D on electrochemical storage systems in the Materials Department since 2007. He joined IFP with an Engineering degree of the Grenoble Electrochemistry National School (ENSEEG) and a PhD in Electrochemistry.

Engineer of the Applied National School of Lyon (INSA), **Joseph Martin** develops and operates specific testing benches at IFP over 20 years. He is responsible of the 500A/500V power bench in the Materials Department of IFP Lyon.

IFP Expert in Control - hybrid vehicles, **Antonio Sciarretta** is researcher, lecturer and teaching coordinator in the Computer Science Department of the Technology, Computer Science and Applied Mathematics Division. He joined IFP in 2006 with a PhD in thermal machines (University of L'Aquila, Italy).

Youssef Touzani joined the Control, Signal Processing, Real-Time Computing Department of the Technology, Computer Science and Applied Mathematics Division in 2007 with a PhD in power electronics. He develops testing benches to validate new control strategies.

Jean-Charles Dabadie is in charge of R&D in model and simulation in the Engine CFD and Simulation Department of the Energy Applications Techniques Division.

IFP Expert Director in Hybrid vehicles, **François Badin** joined the Engines Laboratory Department of the Energy Applications Techniques Division in 2008.